ANALYTICAL MODELING OF QUALITY FACTOR FOR SHELL TYPE MICROSPHERE RESONATORS

R. Talebi[1], K. Abbasian[1, *], and A. Rostami[1, 2]

[1]School of Engineering-Emerging Technologies, University of Tabriz, Tabriz 51666, Iran

[2]Photonics and Nanocrystal Research Lab. (PNRL), Faculty of Electrical and Computer Engineering, University of Tabriz, Tabriz 51666, Iran

Abstract—In this paper, we have proposed a shell type dielectric microsphere resonator in order to enhance its quality factor. In this work we have assumed that the radius of dielectric microsphere is 12 µm and that the interior metal layer radius is 11.5 µm. We have obtained analytic equations for Vector potentials, characteristic equation, quality factor, resonance frequency and resonance location of TE modes. We have plotted these characteristics by MATLAB software and compared them with the normal microsphere characteristics.

1. INTRODUCTION

Dielectric microspheres as high quality factor (high-Q) resonators with whispering gallery modes (WGM's) are a novel type of optical resonators. These are going to become more and more attractive in nowadays applications. The high quality factor and small effective mode volume of dielectric cavities make them extremely well suited to cavity quantum Electrodynamics (cavity QED) experiments [1]. Enhanced spontaneous emission has been observed from semiconductor nanocrystals embedded in polystyrene spheres [2]. A high-Q silica microsphere/nanocrystal system has also been demonstrated which may lead to realization of the strong-coupling regime of cavity QED for atoms and semiconductors [3]. The fused silica microspheres have also been developed for commercial applications such as add/drop filter [4] and a sensor for detection of trace-gas [5] and biological

molecules [6]. WGMs can be used as efficient and compact optical switches and modulators. A possibility of nonlinear optical switching and applications of WGRs to create a quantum-mechanical computer was first recognized in [7]. Whispering gallery modes first were observed by acoustic waves in ancient places like as Peking (the temple of sky) or in London (St. Paul's cathedral), etc. [8]. These waves were supposed to be conveyed by something invisible through the circular building (almost stone ones) and returning back to the opposite side of their uttered place. Later the modern physical explanation of this effect was proposed by Rayleigh as early as over a century ago [9]. Optical WGM's were first observed in scattering experiments by Mie, and WGMs are therefore often referred to as "Mie Resonances" [10, 11]. However, it was not until recent decades that utilizing these unique modes in optic and photonic devices have been practically experimented. Electro Magnetic (EM) waves in micro resonators (like as microspheres) act in similar way the acoustic waves action in circular building. The WGMs ability to store and build up optical energy is the main reason of using this structure widely. A high-Q microsphere can confine Whispering gallery modes by total internal reflection on the cavity interface. The storage time of photons in these modes in silica microspheres can exceed a microsecond [12]. The large amount of resonant power build up in high-Q microspheres means that, if the input coupling power to the microsphere is 1mw, with a Q-factor around 100 million(which was already achievable) we can have the circulation power on the order of 100 Watts in very small volume [12]. Increasing the quality factor can be useful in some branches like as lasing and nonlinear optics [7], so that we can have a very low input power (very low threshold). In order to improve the quality factor of microsphere, we have proposed a shell type structure microsphere. It has been analytically demonstrated that its Q-factor can be improved considerably. Generally, the overall quality factor of a whispering gallery mode cavity is limited by several factors [13–15]:

$$1/Q_{\text{total}} = 1/Q_{\text{mat}} + 1/Q_{\text{WGM}} + 1/Q_{\text{ss}} + 1/Q_{\text{contam}} + 1/Q_{\text{coupling}}$$
$$= 1/Q_{\text{intrinsic}} + 1/Q_{\text{coupling}},$$

where, (Q_{total}) denotes the total cavity quality factor. The intrinsic quality factor $Q_{\text{intrinsic}}$ is due to contributions from both microsphere material losses (Q_{mat}), radiation loss present in a curved dielectric cavity (Q_{WGM}), scattering from surface imperfections (Q_{ss}) and any contaminate on either cavity surface or inside the dielectric (Q_{contam}). Q_{coupling} represents the energy loss due to the input/output coupling. In this paper, we want to improve Q_{WGM} of microsphere to the ultimate level determined by fundamental material attenuation. As other loss factors (except the coupling loss) are well-known for the high purity

silica microsphere. The objective of this paper is to highlight analytic investigation of shell type structure microsphere and calculating its ultimate WGM's quality factor. At first part of Section 2, the fields associated a normal microsphere and WGM's quality factors of a normal microsphere have been highlighted. Then analytic formulas, the characteristic equation and the resonance location of our proposed system have been derived. In Section 3, the simulation results of both structures have been brought and compared with each other.

2. THEORY BACKGROUND

2.1. Normal Microspheres

To explain modes and fields in a shell type structure microsphere, first it is necessary to have a view of normal microspheres. In Figure 1, a sphere and zig-zag propagating mode around equatorial plane has been shown. The coordinates of sphere are presented by the usual variables, r for the radial direction, φ for the azimuthally direction, and θ for the polar direction. Due to orthonormality of the variables, the fields of the sphere can be separated as

$$\Psi_{l,m,n}(r, \Theta, \Phi) = \Psi_r(r)\Psi_\theta(\Theta)\Psi_\varphi(\Phi), \tag{1}$$
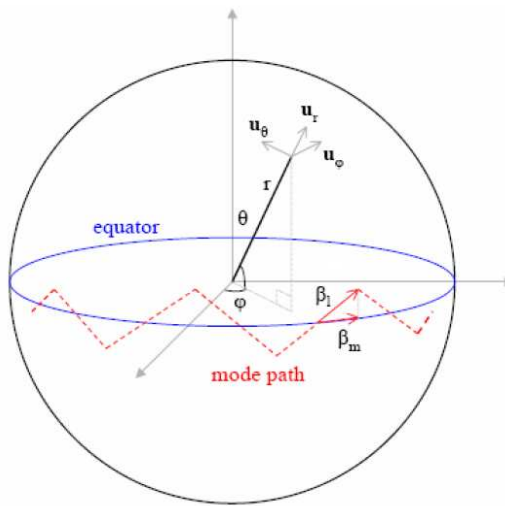

Figure 1. Spherical coordinate system for whispering-gallery modes propagation along the surface of the sphere.

where as shown in numerous references the component contributions take the form [15, 17]

$$\Psi_r(r) = \begin{cases} j_l(k_0 n_s r), & r \le a \\ h_l(k_0 r), & r > a \end{cases} \qquad (2)$$

$$\Psi_\theta(\Theta) = p_l^m(\cos(\theta)) \qquad (3)$$

$$\Psi_\Phi(\Phi) = \exp[jm\varphi], \qquad (4)$$

where $\Psi_{l,m,n}(r,\Theta,\Phi)$ represents either the E_θ or H_θ component of the electromagnetic field. The field components include the following components.

1) The azimuthal contribution ψ_φ with integer mode number $|m| \le l$.

2) The polar contribution Ψ_θ which is often expressed in terms of exact solutions, the associated Legendre Polynomials $P_m^l(\cos(\theta))$.

3) The radial contribution Ψ_r comprised of spherical Bessel functions interior to the sphere. Exterior to the sphere, but very close to the surface, the fields decay exponentially [17]. (Also exterior to the sphere the radial components can be presented by spherical Hankel functions [12, 18].)

A sphere mode is conventionally described in terms of three integer set (l, m, n). l is the azimuthally mode number and is equal to the number of wavelengths taken to travel around the sphere for a particular resonance mode. For a particular value of l, there are many solutions due to the form of the spherical Bessel function $j_l(kr)$, and each one corresponds to a different radial mode number, n, with n being equal to the number of intensity maxima in the radial direction. The final, polar with mode number of m, describes the field variation in the Polar direction, with $l - |m| + 1$ number of intensity maxima. So that the "fundamental" mode has $l = m$ and $n = 1$. Modes with the same values of l and n but different values of m are degenerate but, having different field distributions, will have different waveguide coupling factors and, hence, Q-factors [17, 19]. The characteristic equation which describes the relation between the wave vector k_0 and the eigenvalues l and n, is determined by matching tangential electric and magnetic fields across the surface $r = a$.

Two independent cases are identified as consequences of separation solutions: 1) Transverse electric (TE) modes, where the electric field is parallel to the surface. The vector components are $\vec{E} = \widehat{\theta} E_\theta = \widehat{\theta} \Psi_{l,m,n}$, $E_\varphi = E_r = 0.2$) Transverse magnetic modes (TM), where the magnetic field is parallel to the surface. The vector components are $\vec{H} = \widehat{\theta} H_\theta = \widehat{\theta} \Psi_{l,m,n}$, $H_\varphi = H_r = 0$. The remaining H fields of the TE modes, or the E fields of the TM modes, are derived by Maxwell's

equations. Matching tangential fields lead to simple characteristic equation [13, 17].

$$n_s^{1-2c} \frac{j_{l-1}(n_s k_0 a)}{j_l(n_s k_0 a)} = \frac{h_{l-1}^{(2)}(k_0 a)}{h_l^2(k_0 a)} \tag{5}$$

where 'c' represents the polarization of the optical mode (1 for TM and 0 for TE) and 'a' is the radius of the sphere and this equation is obtained by imposing $r = a$ at the surface of the sphere, $k_0 = 2\pi/\lambda$ is the wave vector outside of the sphere, by considering air as the surrounding medium and then $K = n_s 2\pi/\lambda$ is the wave vector inside the sphere, n_s is the refractive index of the sphere and l is a quantum number which has been described already. These characteristic equations determine in fact the relation between the wave number K and the sphere radius 'a'.

Factors $j_l(n_s k_0 a)$ and $h_l(k_0 a)$ are the first order spherical Bessel and Hankel functions, respectively [16]. The spherical Bessel and Hankel functions are easily computed by using recursion formula [17] or can be computed by using the relation [7, 16]:

$$j_l(kr) = \sqrt{\pi/2kr} J_{l+1/2}(kr) \tag{6}$$

where $j_l(kr)$ represents spherical Bessel function and $J_l(kr)$ represents ordinary Bessel function.

Solution of characteristic equation results in a complex wave vector, $k = k_r + ik_i$, which determines both the resonance wavelength ($\lambda = 2\pi k_r$) and the radiation quality factor ($Q_{\mathrm{WGM}} = k_r/(2k_i)$) [12]. While the radiation loss can easily be found by solving the characteristic equation (as mentioned above), a simple approximated expression can be used to gain insight into the scaling of radiation loss as a function of the cavity parameters [12, 18].

$$Q_{\mathrm{WGM}} = 1/2(l+1/2)n_s^{1-2c}(n_s^2 - 1)^{1/2}e^{2T_l} \tag{7}$$

where

$$T_l = (l+1/2)(\eta_l - \tanh \eta_l) \tag{8}$$

$$\eta_l = ar \cosh \left\{ n_s \left[1 - (1/l+1/2) \left(t_q^0 \zeta + \frac{n_s^{1-2c}}{\sqrt{n_s^2 - 1}} \right) \right] \right\}^{-1} \tag{9}$$

$$\zeta = (1/2(l+1/2))^{1/3} \tag{10}$$

$$c = \{1(\mathrm{TM}), 0(\mathrm{TE})\} \tag{11}$$

where l is the azimuthally mode number, n_s is the refractive index of sphere, c is the polarization of the optical mode and t_q^0 is the qth zero of Airy function [20] (Table 1). We observed that the quality factor of a microsphere depends on its refractive index, quantum number l and the radius of the sphere.

Table 1. The first 15 roots of the equation $A_i(t) = 0$.

q	t_q
1	-2.338
2	-4.088
3	-5.521
4	-6.787
5	-7.944
6	-9.023
7	-10.040
8	-11.009
9	-11.936
10	-12.829
11	-13.692
12	-14.528
13	-15.341
14	-16.133

2.2. Shell Type Structure Microsphere

In many applications it is desired to improve quality factor of a microsphere. So in the first step, we have explored multilayer structure to catch our goal. Since better results depend on the confinement of whispering gallery modes nearer the surface, it has been concluded that the refractive index of an interior sphere must satisfy the condition: $N_1 < n_s$ so that it acts as a clad in optical fibers. It is useful here to mention that in a Normal microsphere, high order modes penetrate more than fundamental mode to the center of sphere and it is not useful. Only the modes those are pressed to the surface of sphere have the miraculous effects of WGMs.

Then the best proposed material for interior sphere has seemed to be a metal. On the interface between silicon and metal something like as total internal reflection happens on the surface of metal, as a result, the modes are confined between two shields and nearer the surface. Metals don't let the electromagnetic waves go through them. From this discussion two points have been considered, first as modes are not allowed to go inside the metal sphere [16], shell type microsphere (Figure 2) with metal sphere interior to the silica seems to be sufficient
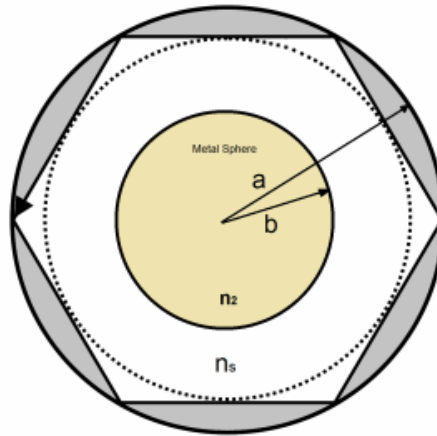
Figure 2. The structure of the proposed shell type microsphere. In this figure, 'a' is the radius of the exterior sphere and 'b' denotes the radius of the interior metal sphere. Here n_2 shows the refractive index of the metal and n_s is the refractive index of the microsphere.

and adequate. The second conclusion is that by changing the metal radius, we can obtain the best quality factor possible for this structure.

For realization of this shell type microsphere, there are some main stages consist of the synthesis of metal cores, the modification of their surfaces with organic materials having functional groups, absorbing of seeding dielectric nanoparticles with diameter of 500 nm on modified cores and the synthesis of dielectric shell by the seeded growth technique [21, 22].

To measure the linewidth of this high Q resonator, we should write that it is somewhat impossible by available lasers. However, one can try it by different optical interferometric approaches with taking required precautions. Where, the optical sources should be ultra-narrow linewidth and tunable Dye lasers to generate nearer modes. Also, the beat note of light sources can show very narrower linewidth [23, 24].

2.3. Characteristic Equation

It is well known that, for an isotropic linear and homogeneous dielectric medium, without any electromagnetic sources inside it, the expressions of electric $\vec{E}$ and magnetic $\vec{H}$ fields can be expressed by the following

equations.

$$\vec{E} = \frac{\nabla \times \nabla \times \vec{A}}{j\omega\varepsilon\mu} - \frac{1}{\varepsilon}\nabla \times \vec{F} \tag{12}$$

$$\vec{H} = \frac{\nabla \times \nabla \times \vec{F}}{j\omega\varepsilon\mu} - \frac{1}{\mu}\nabla \times \vec{A} \tag{13}$$

where, $\vec{A}$ and $\vec{F}$ are called the electric and magnetic potential vectors, respectively [18].

$$A_{1r} = r\Psi(r, \Theta, \Phi) = r(A_1 j_l(n_s k_0 r) + B_1 y_l(n_s k_0 r)).$$
$$P_l^m(\cos(\theta)) \cdot \cos(m\phi) = F_{1r}, \quad b \le r \le a \tag{14}$$
$$A_{2r} = r\Psi(r, \Theta, \Phi) = r(A_2 h_l(k_0 r))$$
$$P_l^m(\cos(\theta)) \cos(m\varphi) = F_{2r}, \quad r > a \tag{15}$$

In these equations we don't have imposed the limitation condition to the second order spherical Bessel function $y_l(kr)$, to be finite at $r = 0$. The characteristic equation which gives us all the information about our resonator has been determined by matching tangential Electric and Magnetic fields at $r = a$.

$$\vec{r} \times \vec{E}_1 \times \vec{r} = \vec{r} \times \vec{E}_2 \times \vec{r} \tag{16}$$
$$\vec{r} \times \vec{H}_1 \times \vec{r} = \vec{r} \times \vec{H}_2 \times \vec{r} \tag{17}$$

Also we require the relationships between A_1, B_1 and A_2. So, we impose the boundary conditions on $r = b$ interface. Also, we would have $E_t = 0$ because the interior material is metal.

Here the relations between A_1, B_1, and A_2 are:

$$B_1 = -A_1 \frac{j_l(k_0 b)}{y_l(k_0 b)} \tag{18}$$

$$A_2 = \frac{\varepsilon_0}{\varepsilon} A_1 \frac{\left(j_l(k_0 r) - \frac{j_l(k_0 b)}{y_l(k_0 b)} y_l(k_0 r) \right)}{h_l(k_0 r)} \tag{19}$$

After mathematical manipulation of these equations and considering this point that in the TE mode the radial component of magnetic vector potential $\vec{A}$ is zero ($A_r = 0$) we can obtain the TE[®] mode characteristic equation.

$$n_s^{1-2c} \left(\frac{j_l'(n_s k_0 r) - D y_l'(n_s k_0 r)}{j_l(n_s k_0 r) - D y_l(n_s k_0 r)} \right) = \left(\frac{h_l'(k_0 r)}{h_l(k_0 r)} \right) \tag{20}$$

where $D = j_l(n_s k_0 b)/y_l(n_s k_0 b)$, and n_s is the refractive index of the microsphere and b is the radius of the interior sphere. Here primes denote the first derivatives of the Bessel and Hankel functions respect to their arguments.

2.4. The Evanescent Whispering Gallery Field in the Shell Type Structure Microsphere

To study the properties of WGMs, first of all we should calculate the roots of the characteristic equations. As we deal with the modes with a large index of l; it is convenient to use the appropriate approximation of the Bessel functions for calculation of these roots. An appropriate approximation should be taken by considering this fact that, the argument of Bessel function for a WGM near the surface is of the order of its index. It is useful to start with some physical insight. For a ray with wave number $n_s k_0$ inside the microsphere striking the microsphere surface at an angle θ to the normal, the angular momentum is [25]

$$v = n_s k_0 a \sin(\theta) = n_s x \sin(\theta) \tag{21}$$

where $\nu = l + 1/2$.

But $\sin(\theta)$ ranges from unity (glancing incidence) to $1/n_s$ (the limit of total internal reflection), thus for large spheres, ν scales with x, and it is therefore convenient to define $\mu = \nu/x(n_s \geq \mu \geq 1)$. Moreover, low order resonance modes (with small quantum number n) correspond to nearly glancing rays, so we expect the absolute value of $|n_s x - \nu|$ to be relatively small; in fact, this difference turns out to scale as $\nu^{1/3}$ [25]. So it is common to define a variable expected to be $O(1)$, by

$$n_s x = \nu + t\nu^{1/3} \tag{22}$$

By these assumptions, the Bessel function can be well approximated by Airy functions [20]:

$$j_l(nx) = (2/\nu)^{1/3} A_i \left(-2^{1/3}t\right) \left[1 + \sum_{j=1}^{\infty} f_j(t)/\left(\nu^{2j/3}\right)\right]$$
$$+ \frac{2^{2/3}}{\nu} A_i' \left(-2^{1/3}t\right) \sum_{j=0}^{\infty} g_j(t)/\left(\nu^{2j/3}\right), \tag{23a}$$

$$j_l'(nx) = -(2/\nu)^{2/3} A_i' \left(-2^{1/3}z\right) \left[1 + \sum_{k=1}^{\infty} h_k(z)/\left(\nu^{2j/3}\right)\right]$$
$$+ \frac{2^{1/3}}{\nu^{4/3}} A_i \left(-2^{1/3}z\right) \sum_{k=0}^{\infty} l_k(z)/\left(\nu^{2k/3}\right), \tag{23b}$$

$$y_l(nx) = -(2/\nu)^{1/3} B_i \left(-2^{1/3} t\right) \left[1 + \sum_{j=1}^{\infty} f_j(t) / \left(\nu^{2j/3}\right)\right]$$

$$-\frac{2^{2/3}}{\nu} B_i' \left(-2^{1/3} t\right) \sum_{j=0}^{\infty} g_j(t) / \left(\nu^{2j/3}\right), \tag{23c}$$

$$y_l'(nx) = (2/\nu)^{2/3} B_i' \left(-2^{1/3} z\right) \left[1 + \sum_{k=1}^{\infty} h_k(z) / \left(\nu^{2k/3}\right)\right]$$

$$-\frac{2^{1/3}}{\nu^{4/3}} B_i \left(-2^{1/3} z\right) \sum_{k=0}^{\infty} l_k(z) / \left(\nu^{2j/3}\right), \tag{23d}$$

And similar expressions can be written down for the Hankel functions. Where $A_i(t)$ and $B_i(t)$ are Pairs of linearly independent solutions of airy function [20].

Inserting the asymptotic expansions into the characteristic equation (main idea of our systematic analysis is illustrated by showing the derivation to first nontrivial order) the two sides of Equation (21) are asymptotically:

$$n_s^{1-2b} \left(-\frac{(2/\nu)^{1/3} \left(A_i' \left(-2^{1/3} t\right) + D B_i' \left(-2^{1/3} t\right)\right)}{A_i \left(-2^{1/3} t\right) + D B_i \left(-2^{1/3} t\right)}\right)$$
$$= \sqrt{\mu^2 - 1} \left(1 - i \exp(-2T_l)\right) \tag{24}$$

which by taking $\nu \to \infty$ with μ fixed ($n \geq \mu \geq 1$), we see that the powers of l can only balances if

$$A_i \left(-2^{1/3} t\right) + D B_i \left(-2^{1/3} t\right) = O(\nu^{-1/3}) \to 0 \tag{25}$$

We named 't', which satisfies this equation t_0^p.

So, unlike the normal microsphere, the resonance locations in shell type structure are not just related to the roots of airy function ($A_i(t)$). Here these locations depend both to the Airy functions ($A_i(t), B_i(t)$) and also to other factors such as interior sphere's radius. These parameters give us two freedom degrees to control the resonance locations.

We have observed in analytic equations of the quality factor for a normal microsphere that by changing the qth root of Airy function, the quality factor changes rapidly. For example as it is shown in Table 2, in a microsphere by refractive index $n_s = 1.36$ and radius $a = 10\,\mu$m, the quality factors for the first and second roots of Airy function, for respective $l = 128$ and $l = 121$, are $Q = 5 \times 10^{13}$ and $Q = 4 \times 10^9$, respectively [26]. This process will continue for the other successive
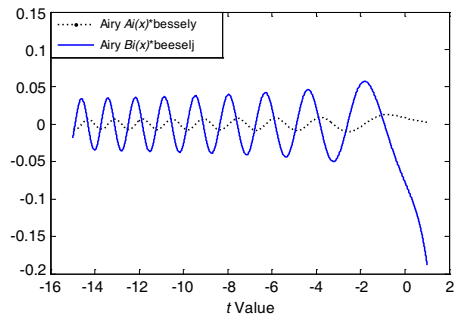
Figure 3. Plot of $t'_p s$ for a shell type microsphere with, $a = 12\,\mu\text{m}$, $b = 11.5\,\mu\text{m}$, and $n_s = 1.36$.

roots of airy function, to control the value of quality factor. By the proposed system we can handle the quality factor. This fact shows the advantage of the our proposed system. The values of the first 15 roots of Equation (26) for the shell type microsphere structure by radii, $b = 11.5\,\mu\text{m}$ and $a = 12\,\mu\text{m}$, and the refractive index for exterior sphere $n_s = 1.36$ has been brought in the Table 3. Also a plot of these roots for the mentioned structure is shown in Figure 3.

Quality factor of the proposed structure can be obtained analytically either by the above mentioned equations (for the normal microsphere in the Section (2.1), and bearing in mind that now instead

Table 2. The values of quality factor of a microsphere, by refractive index $n_s = 1.36$ and radius, $a = 10\,\mu\text{m}$. The Value of Q for $q = 1$, 2, 3 decreases rapidly, respectively.

L	c	q	Q_{WGM}
128	0	1	5×10^{13}
121	0	2	4×10^{9}
115	0	3	6×10^{6}
127	1	1	3×10^{13}
120	1	2	3×10^{9}
114	1	3	5×10^{6}

Table 3. First 15th roots (t_q) of the equation: With $b = 11.5\,\mu\mathrm{m}$.

p	t_p
1	-1.0601
2	-2.6784
3	-3.09021
4	-4.9573
5	-5.9101
6	-6.7915
7	-7.6190
8	-8.4038
9	-9.1536
10	-9.8738
11	-10.5686
12	-11.2413
13	-11.9844
14	-12.5301
15	-13.1500

of t_q we must use the t_p), or by following equations:

$$Q = \frac{\nu - \left(\frac{\nu}{2}\right)^{1/3} t_p - \frac{n_s^{1-2c}}{\sqrt{n_s^2-1}}}{\frac{n_s^{1-2c}}{\sqrt{n_s^2-1}}} \times (\exp(-2T_p)) \qquad (26)$$

where $\nu = l + 1/2$ and T_p can be calculated from

$$T_p = (l + 1/2)(\eta_l - \tanh\eta_l) \qquad (27)$$

where, η_l can be obtained from Equation (9) with replacing t_q by t_p. Δt_p relation with η_l can be obtained by the equation:

$$\Delta t_p = \frac{n_s^{1-2c}\left(\frac{2}{\nu}\right)^{1/3}}{\sqrt{\mu^2 - 1}}(1 + i\exp(-2T_p)) \qquad (28)$$

One way to represent the resonance frequency of this structure is

$$w = \frac{c}{an_s}\left[l + 2^{-1/3}t_p^0 l^{1/3} + \frac{n_s^{1-2b}}{\sqrt{n_s^2 - 1}}(1 + i\exp(-2T_p)) + O(1)\right] \qquad (29)$$

By mathematical manipulating of above equations, the resonance locations for this structure can be given by following equation:

$$x = \frac{1}{n_s} \left(\nu + 2^{-1/3} \left(t_p + \Delta t_p \right) \nu^{1/3} + O(1) \right) \tag{30}$$

where, Δt_p has been given by Equation (28).

3. THEORETICAL RESULTS AND CONCLUSIONS

3.1. Normal Microsphere

In this section, the discussed formulas for a normal microsphere and also the derived formulas for the shell type microsphere have been used or plotted to examine the trends in Q factor as a function of various parameters. In the most of the following graphs, there are four curves. In the $n = 1$ labeled curves (red color), the WGM is strongly confined in a thin superficial layer. For this reason the effect of the spherical bounding is not so strong on the propagation of this mode and the quality factor is the highest. On the other hand, by maintaining fixed the value of related parameters and increasing n, we can observe a decrease of radiative quality factor Q_{WGM}. This is due to the fact that, for higher values of quantum number n, the radial part of the field presents an increase of maxima in this direction and the mode extends towards deeper regions in the microsphere and the curvature effect is more strength on it. For $n = 2$ labeled curves (green color), the WGM has two maxima in the radial direction and it penetrates more than the first case, $n = 1$, to the center of sphere and so the quality factor will decrease. The same process continues for the $n = 3$ case
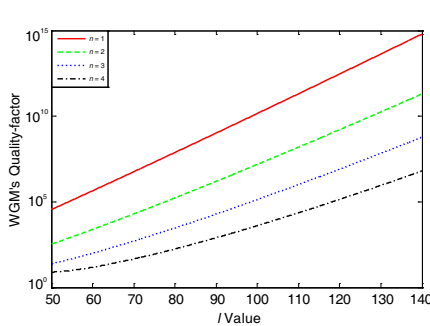

Figure 4. Quality factor of normal microsphere as a function of quantum number l with $n_s = 1.36$ and $a = 10\,\mu\text{m}$.
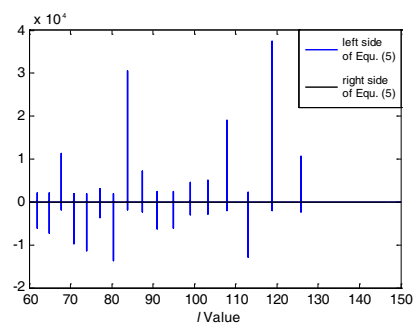
Figure 5. Possible amounts of quantum number l for a normal dielectric microsphere with $a = 16\,\mu\text{m}$, $n_s = 1.985$ and $\lambda = 1480\,\text{nm}$.

(blue color), and become the worst for $n = 4$ case (black color). As it has been shown in Figure 4, Quality factor of a normal microsphere increases as the quantum number l increases. This diagram discloses this fact that for a sphere, maximum quality factor happens, (for the fundamental mode $n = 1$), when l posses the maximum possible value. As it can be seen in the Figure 4 for the fundamental mode, $n = 1$, of a microsphere with the radius $a = 10\,\mu$m, refractive index $n_s = 1.36$, the quality factor for $l = 100$ gets $Q = 1.43 \times 10^{10}$, and for quantum number $l = 128$, become 2.7×10^{13}. The possible exact values of quantum number l for a normal dielectric microsphere can be obtained by solving the characteristic equation of microsphere numerically. Figure 5, shows the possible values of quantum number l for a sphere.

With radius $a = 16\,\mu$m, refractive index $n_s = 1.985$, $\lambda = 1480\,$nm (Here these values has been selected to be compared with some references [18]). Discrete values of quantum number l are 125, 118, 113, 107, 103, 99, 95, 91, 87, 83, 80, 77, 74, 70 and 67 which are closed to those reported in [17].

Figure 6 shows the radiation quality factor of a normal dielectric microsphere as a function of refractive index, n_s. This diagram reveals that for a sphere, quality factor increases as the refractive index of the microsphere increases [17]. As a result, for the fixed quantum numbers l, and the sphere radius a, maximum quality factor occurs for a microsphere which has the highest refractive index possible. It can be seen from Figure 6, that for the $n = 1$ case of a microsphere with $a = 10\,\mu$m and $n_s = 1.36$ the value of quality factor is $Q = 1.13 \times 10^{13}$, but for this situation when the refractive index become, $n_s = 1.6$, the
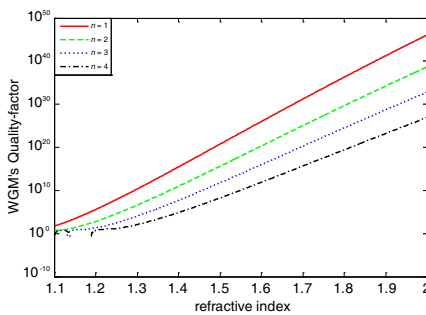

Figure 6. Quality factor as a function of the refractive index n_s for a microsphere with $a = 10\,\mu$m.
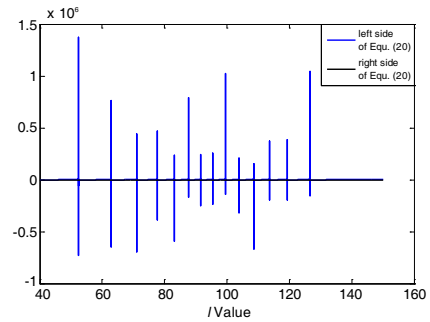
Figure 7. Possible values of the quantum number l for the TE mode of the shell type structure microsphere.

quality factor will be $Q = 2.3 \times 10^{25}$. Increasing of quality factor by refractive index increasing is in result of this fact that when the index contrast between the sphere index and the surrounding medium increases, the confining of light inside the sphere become stronger, therefore the quality factor increases [17].

3.2. Shell Type Structure Microsphere

Like as what have been done for a normal microsphere the set of l values that satisfies characteristic equation of TE mode can be obtained from numerical solving of the characteristic equation. Figure 7, shows the possible values of quantum number l for the proposed shell type structure with radii $a = 16 \,\mu\text{m}$ and $b = 1 \,\mu\text{m}$, refractive index $n_s = 1.985$, and $\lambda = 1280 \,\text{nm}$. These parameters have been used to compare the results with the normal dielectric sphere. The discrete values of the used values for the quantum Number l are 127, 120, 114, 109, 102, 98, 93, 88, 83, 78 and 75.

Figure 8 shows that, like as what have been seen for the normal microsphere, quality factor increases with the increasing of the quantum number l for the shell type microsphere. Similar to the normal sphere case, here in the shell type structure, maximum quality factor for a sphere with known radii and dielectric refractive index happens for the fundamental mode ($n = 1$). As it can be seen in Figure 7, for the fundamental mode of a sphere with radii $a = 12 \,\mu\text{m}$ and $b = 11.5 \,\mu\text{m}$, when $l = 100$, quality factor becomes $Q = 4.45 \times 10^{12}$, and for $l = 127$, quality factor becomes $Q \approx 1.03 \times 10^{16}$. And it is obvious that increasing the value of l will result in increasing of the quality factor.

Comparing the results of quality factor for shell type structure with normal one, for mentioned radii and refractive index, it can be found that quality factor has been improved considerably. As it was illustrated in Figures 6 and 9, by increasing the refractive index of the sphere its quality factor increases. Therefore, to gain higher quality factors it is desired to increase the refractive index as much as possible. As in the normal sphere, the refractive indices of materials used to form a sphere are limited, by selecting the shell type microsphere and handling the radius and material of metal, we can get quality factors which are analog to the high refractive index normal microsphere.

Last discussion can be better revealed in Figure 9. It shows the quality factor of the shell type structure microsphere as a function of its dielectric refractive index (n_s). It could be predicted that quality factor of this structure will increase by increasing of its refractive index too. It has been illustrated that for the fundamental mode ($n = 1$) of the shell type microsphere with radii, $a = 12 \,\mu\text{m}$, $b = 11.5 \,\mu\text{m}$, and
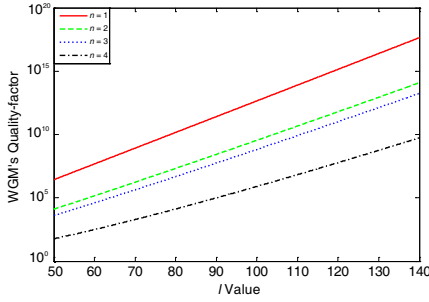
Figure 8. Quality factor of the shell type microsphere as a function of the quantum number l with $n_s = 1.36$, $a = 12\,\mu\text{m}$ and $b = 11.5\,\mu\text{m}$.
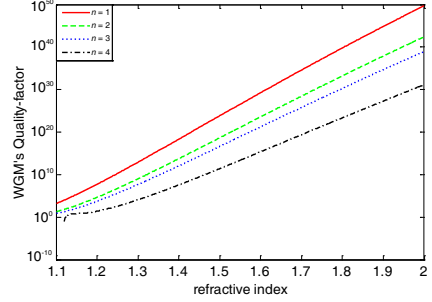
Figure 9. Quality factor of the shell type microsphere as a function of the refractive index n_s with $a = 12\,\mu\text{m}$ and $b = 11.5\,\mu\text{m}$.

dielectric refractive index $n_s = 1.36$, we obtain the radiative quality factor of $Q \approx 1.03 \times 10^{16}$ and when $n_s = 1.6$, quality factor becomes $Q \approx 1.05 \times 10^{29}$. Comparing these results with those for a normal sphere verifies the considerable improving of quality factor for this structure. The quality factor for this structure with the dielectric refractive index $n_s = 1.36$, and for the normal microsphere with refractive index $n_s = 1.415$ are approximately equal.

4. CONCLUSIONS

Analytic equations have been developed for Whispering gallery mode quality factor of the proposed shell type microsphere. For this means, electric and magnetic potential vectors of this structure have been discussed. Then its Characteristic equation has been obtained and a discrete set of quantum numbers l have been given to satisfy characteristic equation. By analytic formulas of the normal dielectric microsphere, it has been demonstrated that whispering gallery mode quality factor depends strongly to the roots location of the Airy function, $A_i(t)$. As the root number 'qth' of airy function increases, quality factor decreases rapidly. Therefore, always the first root of the Airy function will give us the highest ultimate quality factor of the microsphere. This fact made us to search if it is possible to change the location where the first zero of Airy function happens. Then it was found that by using a shell type microsphere with metal sphere interior to the dielectric exterior sphere, it is possible to handle locations of Airy function which here are calculating from a combination of the

Airy functions A_i and B_i. Then by changing radii of the metal and dielectric spheres we were able to change the roots of combination of Airy functions and handling the value of quality factor. As a result, considerable improvement of the quality factor has been demonstrated. The diagrams of the shell type microsphere showed us that this structure with lower dielectric sphere refractive index can replace a normal microsphere with a higher refractive index to obtain a given quality factor. Higher refractive contrast between normal sphere and its surrounding medium is desired to better confinement of photons and as a result to obtain higher radiation quality factor. Also because we have tradeoff between loss parameters and coupling to and from the microsphere, in the normal microsphere, if we choose the sphere with the bigger radius, we will have better confinement of photons and as a result loss parameters will decrease and the quality factor will improve but in this situation coupling will decrease. So in the normal microsphere we are limited to a radius which we have both parameters acceptable. Now by this proposed structure, in practical situations we can choose smaller spheres with the same quality factor, while we will have better coupling to and from the shell type microsphere. Another benefit of using this structure is that in normal spheres, for higher order modes, fields penetrate to the center of sphere and this is not desired. By this structure we prevent high order modes to go through the center of sphere (because the interior layer is metal) and will confine them in the shield between two spheres which is one of our goals of using this structure (only modes which are confined to the surface of the microsphere are WGMs). Coupling from tapered fibers to and from our proposed structure and comparing the analytic results and numerical results are the subject of the next publication.

REFERENCES

1. Vernooy, D. W., V. S. Ilchenko, H. Mabuchi, E. W. Streed, and H. J. Kimble, "High-Q measurements of fused-silica microspheres in the near infrared," *Optics Letters*, Vol. 23, No. 4, 247–249, February 1998.

2. Fan, X., M. C. Lonergan, Y. Zhang, and H. Wang, "Enhanced spontaneous emission from semiconductor nanocrystals embedded in whispering gallery optical microcavities," *Phys. Rev. B*, Vol. 64, 115310, 2001.

3. Fan, X., S. Lacey, P. Palingilins, H. Wang, and M. C. Lonergan, "Coupling semiconductor nanocrystals to fused silica microspheres: A quantum-dot microcavity with extremely high Q-factor," *Optics Letters*, Vol. 25, 1600, 2000.

4. Cai, M., G. Hunziker, and K. J. Vahala, "Fiber-optic add-drop device based on a silica microsphere-whispering gallery mode system," *IEEE Photonics Technology Letters*, Vol. 11, 686, 1999.

5. Rosenbeger, A. T. and J. P. Rezac, "Whispering-gallerymode evanescent-wave microsensor for trace-gasdetection," *Proc. SPIE*, Vol. 4265, 102–112, 2001.

6. Arnold, S., M. Khoshisma, I. Teraoka, S. Holler, and F. Vollmer, "Shift of whispering-gallery modes in microspheres by protein adsorption," *Optics Letters*, Vol. 28, 272, 2003.

7. Braginsky, V. B., M. L. Gorodetsky, and V. S. Ilchenko, "Quality-factor and nonlinear properties of optical whispering-gallery modes," *Phys. Lett. A*, Vol. 137, 393–397, 1989.

8. Strutt, J. W., (Lord Rayleigh), *The Theory of Sound*, Dover Press, New York, 1945.

9. Strutt, J., (Lord Rayleigh), *Theory of Sound (Teoriya Zvuka)*, Vol. 2, Gostekhizdat, Moscow, 1955.

10. Mie, G., "Beitrage zur optik truber Medien, speziell kolloidaler Metallosungen," *Ann. Phys.*, Vol. 25, 377–445, Leipzig, 1908.

11. Kerker, M., "The Scattering of light and other electromagnetic radiation," *Academic*, New York, 1969.

12. Spillane, S. M., "Fiber-coupled ultra-high-Q microresonators for nonlinear and quantum optics," Doctor of Philosophy Thesis, May 25, 2004.

13. Vernooy, D. W., V. S. Ilchenko, H. Mabuchi, E. W. Streed, and H. J. Kimble, "High-Q measurements of fused-silica microspheres in the infrared," *Optics Letters*, Vol. 23, 247–249, 1998.

14. Gorodetsky, M. L. and V. S. Ilchenko, "High-Q optical whisperinggallery microresonators: Precession approach for spherical mode analysis and emission patterns with prism couplers," *Opt. Comm.*, Vol. 113, 133–143, 1994.

15. Collot, L., V. Lefevre-Seguin, M. Brune, J. M. Raimond, and S. Haroche, "Very high-Q whispering-gallery mode resonances observed on fused-silica microspheres," *Europhys. Lett.*, Vol. 23, No. 5, 327–334, August 1993.

16. Jackson, J. D., *Classical Electrodynamics*, 3rd Edition, John Wiley & Sons, Inc., 1999.

17. Little, B. E., J. P. Laine, and H. A. Haus, "Analytic theory of coupling from tapered fibers and half-blocks into microsphere resonators," *Journal of Lightwave Technology*, Vol. 17, No. 4, April 1999.

18. Berneschi, S., "Microlaser in rare earths doped glasses," Degree

of Doctor of Philosophy Thesis, Anno Accademico, 2005–2006.

19. Collot, L., V. Lefevre-Seguin, M. Brune, J. M. Raimond, and S. Haroche, "Very high-Q whispering-gallery mode resonances observed on fused silica microspheres," *Europhys. Lett.*, Vol. 23, 327–334, 1993.

20. Abramovitz, M. and I. A. Stegun, *Handbook of Mathematical Functions*, Vol. 55, National Bureau of Standards Applied Mathematics Series, Washington, D.C., 1972.

21. Mine, E., A. Yamada, Y. Kobayashi, M. Konno, and L. M. Liz-Marzán, "Direct coating of gold nanoparticles with silica by a seeded polymerization technique," *Journal of Colloid and Interface Science*, Vol. 264, No. 2, 385–390, 2003.

22. Graf, C., D. L. J. Vossen, A. Imhof, and A. V. Blaaderen, "A general method to coat colloidal particles with silica," *Langmuir*, Vol. 19, No. 17, 2003.

23. Yu, Y., G. Giuliani, and S. Donati, "Measurement of the linewidth enhancement factor of semiconductor lasers based on the optical feedback self-mixing effect," *IEEE Photonics Technology Letters*, Vol. 16, No. 4, 2004.

24. Liu, T., Y. H. Wang, R. Ddumke, A. Stejskal, Y. N. Zhao, J. Zhang, Z. H. Lu, L. J. Wang, T. Becker, and H. Walther, "Narrow linewidth light source for an ultraviolet optical frequency standard," *Appl. Phys. B*, Vol. 87, 227–232, 2007.

25. Lam, C. C., P. T. Leumg, and K. Young, "Explicit asymptotic formulas for the positions, width and strength of resonances in the mie scattering," *J. Opt. Soc. Am. B*, 1585, 1992.

26. Datsyuk, V. V., "Some characteristic of resonant electromagnetic modes in a dielectric sphere," *Appl. Phys. B*, Vol. 54, 184–187, 1992.